JACS Au
AN OPEN ACCESS JOURNAL OF THE AMERICAN CHEMICAL SOCIETY

pubs.acs.org/jacsau

Article

Synthesis of an Adaptable Molecular Barrel and Guest Mediated Stabilization of Its Metastable Higher Homologue

Ranit Banerjee,[‡] Soumalya Bhattacharyya,[‡] and Partha Sarathi Mukherjee*

Cite This: *JACS Au* 2023, 3, 1998−2006

Read Online

ACCESS | Metrics & More | Article Recommendations | Supporting Information

ABSTRACT: Structural and functional modulation of three-dimensional artificial macromolecular systems is of immense importance. Designing supramolecular cages that can show stimuli mediated reversible switching between higher-order structures is quite challenging. We report here construction of a Pd_6 trifacial barrel (**1**) by coordination self-assembly. Surprisingly, barrel **1** was found to exhibit guest-responsive behavior. In presence of fullerenes C_{60} and C_{70}, **1** unprecedentedly transformed to its metastable higher homologue Pd_8 tetrafacial barrel (**2**), forming stable host−guest complexes $(C_{60})_3$⊂**2** and $(C_{70})_2$⊂**2**, respectively. Again, encapsulated fullerenes could be extracted from the cavity of **2** using 1,2-dichlorobenzene, leading to its facile conversion to the parent trifacial barrel **1**. Such reversible structural interconversion between an adaptable molecular barrel and its guest stabilized higher homologue is an uncommon observation.

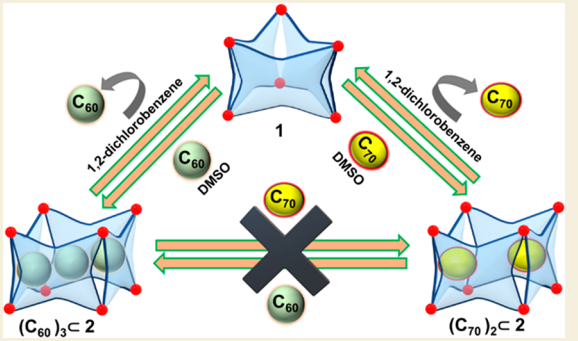

KEYWORDS: *Self-assembly, Molecular barrels, Fullerene encapsulation, Structural transformation, Coordination chemistry*

INTRODUCTION

The flexible and adaptable nature of macromolecular biological receptors is responsible for their structural transformation upon substrate binding. Such flexible and adaptable behavior is mainly due to the noncovalent interactions that drive the biological processes. On the other hand, covalent architectures are generally less prone to structural reorganization to expand their cavity size significantly for better fitting of the substrates. Coordination-driven self-assembly is an efficient technique for designing adaptable large molecular architectures.[1−9] The dynamic nature of the metal−ligand bonding allows for self-correction and conformational changes of the structures.[10−15] The thermodynamically most stable architecture is formed from a given set of building blocks, whereas the other possible geometries remain inaccessible. However, external stimuli[16−30] may induce structural changes to access metastable architectures that are not usually formed. Over the years, the internal cavities of such discrete architectures have been used for binding guest molecules for numerous applications such as catalysis,[31−38] sensing,[39−43] light-harvesting,[44−49] biological applications,[50−52] molecular separations,[53−56] and modification of the dynamics and chemical reactivity of the trapped guests.[57−59] Guest binding within the internal pockets is completely dictated by the size complementarity and favorable noncovalent interactions between the host and the guest. Thus, suitable hosts can be predesigned by incorporating specific functionalities within the building blocks for stabilizing a wide variety of guest molecules within their cavities. Among the various shapes, architectures resembling barrels are expected to be efficient for encapsulating guest molecules due to their large open windows and parallel orientation of the walls which ensures greater interactions with the incoming guest molecules.[60,61]

Fullerenes, due to their interesting physicochemical properties, find applications in several fields.[62−67] The major drawback of working with fullerenes is their poor solubility in common organic solvents. Functionalization of fullerenes to generate soluble derivatives has been the common technique employed to overcome this issue. However, such functionalization usually needs multistep reactions and tedious separation steps.[68] On the other hand, encapsulation of fullerenes within a soluble host is believed to be an easier solution to enhance the solubility of free fullerenes without their chemical modification. Designing suitable receptors that can bind fullerenes in solvents where fullerenes are insoluble has been the prime focus of supramolecular chemists.[69−74] Synthesis of hosts that can encapsulate many molecules of fullerene is highly desirable to enhance their solubility. However, it is a challenging task to

Received: May 5, 2023
Revised: June 4, 2023
Accepted: June 5, 2023
Published: June 19, 2023

design such receptors with large, confined pockets for accommodating more than one fullerene molecule.

Herein, we report the formation of a $[Pd_6L_3]^{12+}$ trifacial molecular barrel (**1**) upon coordination self-assembly (Scheme 1) of a tetratopic ligand **L** with *cis*-$[(tmeda)Pd(ONO_2)_2]$ (**A**)

Scheme 1. Schematic Representation of Synthesis of Trifacial Barrel 1 and Its Conversion to Metastable Higher Homologues in the Presence of C_{60}/C_{70} Molecules

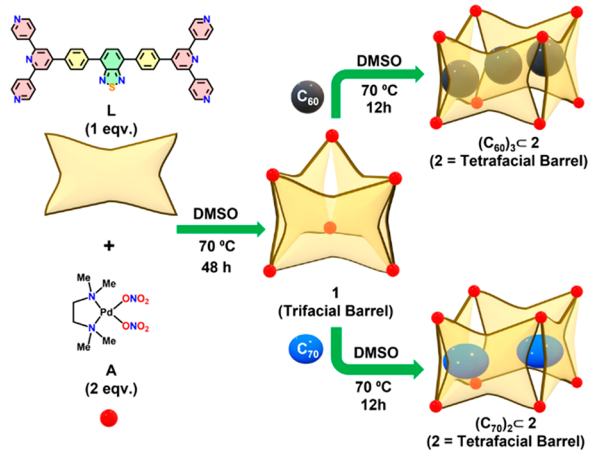

as an acceptor in DMSO (tmeda = N,N,*N*′,*N*′-tetramethylethane-1,2-diamine; DMSO = dimethyl sulfoxide). Trifacial barrel (**1**) possesses a large internal cavity with open windows suitable for encapsulation of large guest molecules. Interestingly, upon treatment with fullerenes C_{60}/C_{70}, the trifacial barrel undergoes an uncommon structural transformation to its higher homologue $[Pd_8L_4]^{16+}$ tetrafacial barrel (**2**) with the formation of fullerene encapsulated stable adducts $(C_{60})_3$⊂**2** and $(C_{70})_2$⊂**2**, respectively. The labile and dynamic nature of the Pd−pyridine bond is ultimately responsible for the transformation of the trifacial barrel to its higher homologue in the presence of external guests to reach its thermodynamically most stable state.[70,75−79] The addition of fullerene to barrel **1** induced reorganization of the building blocks to generate a metastable tetrafacial barrel (**2**) by effective host−guest interactions. Extraction of C_{60}/C_{70} from the host−guest complexes led to facile conversion of **2** to its parent trifacial barrel **1** which indicates that the metastable barrel **2** could only be obtained in the presence of C_{60} or C_{70} as the guest. Such guest-induced reversible structural transformation between homologues of self-assembled molecular barrels and stabilization of a metastable homologue by multiple fullerene molecules are unusual observations. Further, these adducts $[(C_{60})_3$⊂**2** and $(C_{70})_2$⊂**2**] were found to act as photosensitizers for singlet oxygen generation under visible light irradiation in acetonitrile where free C_{60}/C_{70} is insoluble and shows no singlet oxygen generation.

RESULTS AND DISCUSSION

The ligand **L** was synthesized by reacting 4,4′-(benzo[*c*][1,2,5]thiadiazole-4,7-diyl)dibenzaldehyde (**P**) with KOH, 4-acetylpyridine, and NH_4OH in ethanol using a standard procedure for the synthesis of terpyridines.[70,80,81] Precursor **P** was synthesized via Suzuki coupling between 4,7-dibromobenzo[*c*][1,2,5]thiadiazole and (4-formylphenyl)-boronic acid (Scheme S1) following a reported procedure.[82] Self-assembly of **L** and *cis*-$[(tmeda)Pd(NO_3)_2]$ (**A**) was done in a 1:2 molar ratio in DMSO for 48 h at 70 °C which afforded a clear yellow solution (Scheme 1). **1** was isolated as a yellow solid in almost quantitative yield upon addition of excess ethyl acetate to the reaction mixture. ^{1}H NMR of **1** was recorded in DMSO-d_6 which showed downfield shifts of α-pyridyl protons and a 2-fold splitting of α-pyridyl (H_a and $H_{a'}$) and β-pyridyl (H_b and $H_{b'}$) protons of the ligand in comparison to the free **L** due to rigidification of asymmetric ligand **L** upon assembly formation (Figures 1a,b, S1, and S4). All the peaks in the ^{1}H

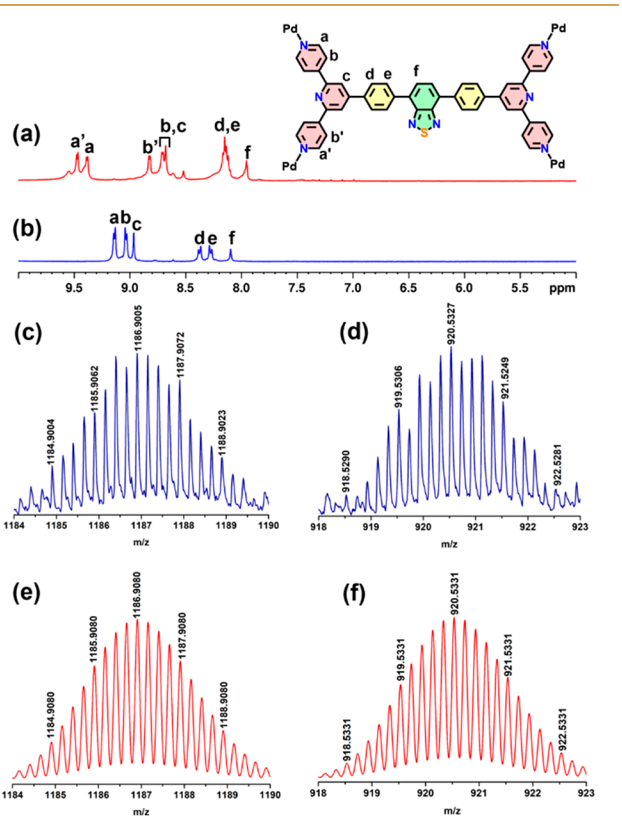

Figure 1. (a) Stacked ^{1}H NMR spectra of **1** and (b) **L** in DMSO-d_6. (c) Experimental (blue) and (e) calculated (red) isotopic patterns of $[\mathbf{1}\text{-}4PF_6]^{4+}$ fragment. (d) Experimental (blue) and (f) calculated (red) isotopic patterns of $[\mathbf{1}\text{-}5PF_6]^{5+}$ fragment in ESI-MS analyses.

NMR spectrum were assigned with the help of ^{1}H−^{1}H COSY (Figure S6) and NOESY NMR (Figure S7). The same diffusion coefficient ($D = 6.025 \times 10^{-11}$ m^2/s) for all the peaks in ^{1}H-DOSY NMR confirmed the formation of a single assembly (Figure S5). **1** was converted to the PF_6^- analogue by treating the nitrate analogue with excess KPF_6 for better ionization. ESI-MS analyses confirmed the formation of a Pd_6L_3 trifacial barrel **1** by the appearance of peaks at m/z = 1630.8743, 1186.9005, 920.5327, and 742.9542 which correspond to the charged fragments $[\mathbf{1}\text{-}3PF_6]^{3+}$, $[\mathbf{1}\text{-}4PF_6]^{4+}$, $[\mathbf{1}\text{-}5PF_6]^{5+}$, and $[\mathbf{1}\text{-}6PF_6]^{6+}$, respectively (Figures 1c,d and S9). The isotopic patterns corresponding to these fragments were in good agreement with the theoretically calculated patterns.

Several attempts to grow single crystals of **1** were fruitless. To gain structural insights, the geometry of **1** was optimized using the PM6 method. In the energy minimized structure of barrel **1**, three tetrapyridyl ligands (**L**) are horizontally oriented in a trigonal disposition and the six corners are clipped by the Pd(II) acceptor **A** (Figure 2). There remains a possibility to obtain an isomeric trifacial tube in which all three ligands are

https://doi.org/10.1021/jacsau.3c00224
JACS Au 2023, 3, 1998−2006

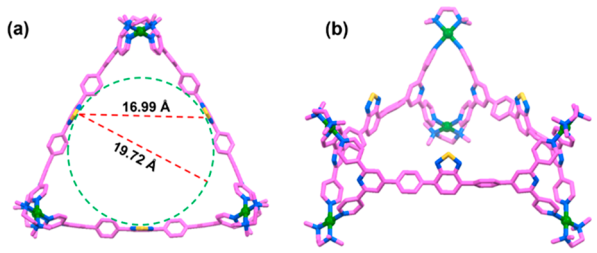

Figure 2. Structure of trifacial barrel **1** obtained by optimization: (a) top view and (b) side view, where ligands are horizontally oriented. Color codes: carbon (pink), nitrogen (blue), sulfur (yellow), and palladium (green). Hydrogen atoms are omitted for clarity.

vertically oriented and clipped to six Pd(II) acceptors. However, the formation of a trifacial tube (Figures S24) is energetically disfavored by about 132 kcal/mol compared to barrel **1** which can be attributed to the greater steric crowding among the vertical panels. From the optimized structure, it is observed that **1** possesses a large internal cavity of diameter 19.72 Å (Figure 2a), π-conjugated aromatic walls, and wide-open windows, suitable for encapsulation and stabilization of large guest molecules.

Fullerenes (C_{60}/C_{70}), on the other hand, are electron-deficient large molecules with negligible solubility in a polar solvent like DMSO. This prompted us to carry out encapsulation of fullerenes C_{60} and C_{70} into barrel **1**. We have recently shown structural conversion of a self-assembled trigonal cage to larger analogue upon binding of large guests like fullerenes.[70] Four equivalents of C_{60} were added to a yellow solution of trifacial barrel **1** in DMSO and stirred at 70 °C for 12 h. The reaction mixture was centrifuged, and a clear brown solution was obtained. The product was isolated as brown solid by treating the solution with excess ethyl acetate. A new set of peaks was seen in the ^{1}H NMR spectrum with downfield shifts of the α-pyridyl protons of the barrel, indicating the formation of a host–guest complex with C_{60} (Figures 3b and S10).

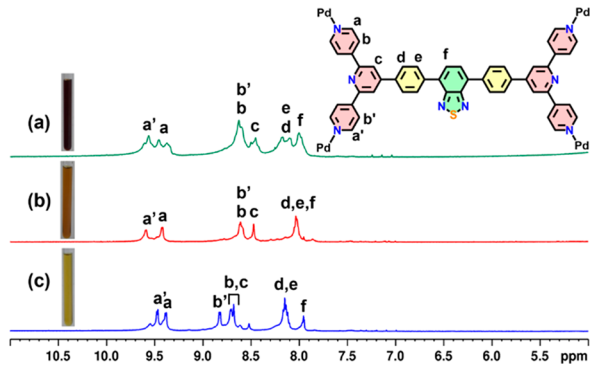

Figure 3. Stacked ^{1}H NMR spectra of (a) $(C_{70})_2$⊂**2**, (b) $(C_{60})_3$⊂**2**, and (c) trifacial barrel **1** in DMSO-d_6. Insets show the color of the solutions.

An encapsulation experiment with the ellipsoidal C_{70} was performed in a similar fashion. A deep-red solution was obtained, which upon treatment with excess ethyl acetate yielded a dark-red solid product. The ^{1}H NMR spectrum of the product was broad due to the presence of unsymmetrical and ellipsoidal C_{70} (Figures 3a and S17). ^{13}C NMR spectra of these complexes were recorded to detect the presence of encapsulated C_{60} or C_{70} molecules. Free fullerenes in DMSO do not show any peak in ^{13}C NMR spectra due to poor solubility. Interestingly, two intense peaks of slightly different intensities were found at δ 141.39 and 140.80 ppm for the C_{60} complex (Figures 4b and S14). Spherically symmetrical C_{60} is

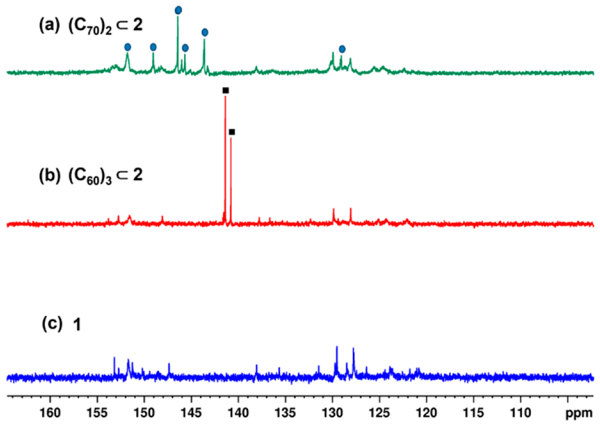

Figure 4. Stacked ^{13}C NMR spectra of (a) $(C_{70})_2$⊂**2**, (b) $(C_{60})_3$⊂**2**, and (c) trifacial barrel **1** in DMSO-d_6.

expected to show a single intense peak in the ^{13}C NMR spectrum. The presence of two peaks hinted toward the possibility of the presence of multiple C_{60} molecules encapsulated within the cavity of the barrel. ^{13}C NMR spectrum of the C_{70} complex showed several intense peaks characteristic of C_{70} which also indicated the possible presence of multiple C_{70} molecules encapsulated within the barrel (Figures 4a and S21).

To get the exact composition of the host–guest complexes, the nitrate analogues were converted to hexafluorophosphates for easy ionization in ESI-MS experimental conditions. Surprisingly, a composition of three C_{60} molecules encapsulated in a homologous tetrafacial barrel **2** ([$(C_{60})_3$⊂**2**]) was found for the C_{60} complex. Peaks were obtained at m/z = 2171.4499, 1708.1593, 1399.3139, 1178.6954, and 1013.2381 which correspond to the charged fragments [$(C_{60})_3$⊂**2**-4PF_6]$^{4+}$, [$(C_{60})_3$⊂**2**-5PF_6]$^{5+}$, [$(C_{60})_3$⊂**2**-6PF_6]$^{6+}$, [$(C_{60})_3$⊂**2**-7PF_6]$^{7+}$, and [$(C_{60})_3$⊂**2**-8PF_6]$^{8+}$, respectively (Figures 5b,d, S15, and S16). The isotopic patterns were in good agreement with theoretically calculated patterns. On the other hand, a composition of two C_{70} molecules encapsulated in a similar tetrafacial barrel **2** ([$(C_{70})_2$⊂**2**]) was obtained for the C_{70} complex from ESI-MS analyses. Peaks and the isotopic distribution patterns were obtained at m/z = 2051.1936, 1611.9548, 1319.1342, 1109.9847, and 953.1152 which correspond to the charged fragments [$(C_{70})_2$⊂**2**-4PF_6]$^{4+}$, [$(C_{70})_2$⊂**2**-5PF_6]$^{5+}$, [$(C_{70})_2$⊂**2**-6PF_6]$^{6+}$, [$(C_{70})_2$⊂**2**-7PF_6]$^{7+}$, and [$(C_{70})_2$⊂**2**-8PF_6]$^{8+}$, respectively (Figures 5a,e, S22, and S23). Interestingly, neither the free trifacial barrel (**1**) nor the tetrafacial barrel (**2**) was detected from mass analyses. Therefore, trifacial barrel **1** undergoes a complete transformation to a homologous tetrafacial barrel **2** with encapsulated C_{60} or C_{70}. While the free tetrafacial barrel was not formed during the reaction, it was isolated in the form of stable host–guest complexes with three C_{60} or two C_{70} molecules.

^{1}H-DOSY NMR confirmed the presence of a single species for both the complexes $(C_{60})_3$⊂**2** and $(C_{70})_2$⊂**2** (Figures S11 and S18). Further, a comparison of the diffusion coefficient

https://doi.org/10.1021/jacsau.3c00224
JACS Au 2023, 3, 1998–2006

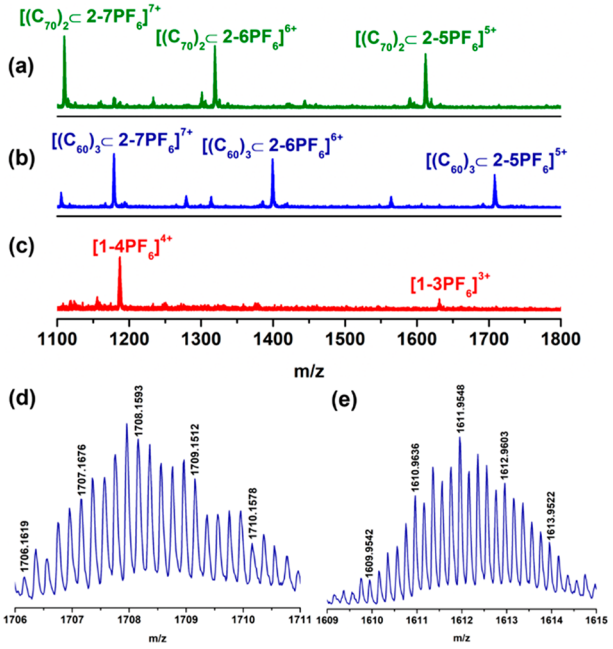

Figure 5. Partial stacked ESI-MS spectra of (a) $(C_{70})_2$⊂**2**, (b) $(C_{60})_3$⊂**2**, and (c) **1**. Experimental isotopic distribution patterns of (d) $[(C_{60})_3$⊂**2**-5$PF_6]^{5+}$ and (e) $[(C_{70})_2$⊂**2**-5$PF_6]^{5+}$ in ESI-MS.

values for the free trifacial barrel **1** (D = 6.025 × 10^{-11} m^2/s) with host–guest complexes $(C_{60})_3$⊂**2** (D = 5.164 × 10^{-11} m^2/s) and $(C_{70})_2$⊂**2** (D = 4.819 × 10^{-11} m^2/s) revealed higher hydrodynamic radii for $(C_{60})_3$⊂**2** and $(C_{70})_2$⊂**2** than the free barrel **1**, which also supports the transformation of **1** to the higher homologue (**2**).

Absorption spectra of **1**, $(C_{60})_3$⊂**2**, and $(C_{70})_2$⊂**2** were recorded (Figure 6) using 10 μM dimethyl sulfoxide solutions

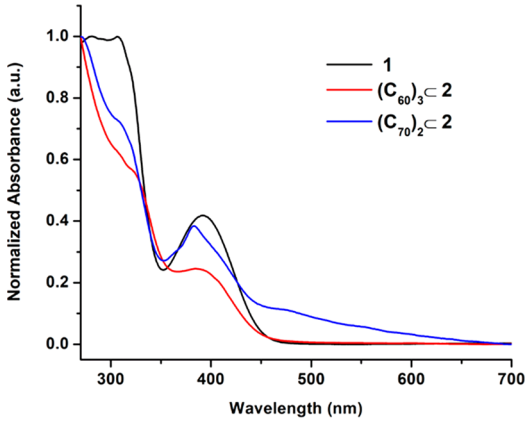

Figure 6. Normalized absorption spectra of **1**, $(C_{60})_3$⊂**2**, and $(C_{70})_2$⊂**2** in DMSO (10 μM concentration).

of the respective complexes. Trifacial barrel **1** displays two absorptions at 307 and 392 nm due to π–π^* transitions. $(C_{60})_3$⊂**2** shows an absorption at 387 nm with a 5 nm blue shift compared to the peak at 392 nm for **1** and a hump at 324 nm (free C_{60} shows an absorption at 321 nm).[83] $(C_{70})_2$⊂**2** shows peaks at 383 and 311 nm and a broad hump at 470 nm (characteristic of C_{70}).[84] These observations further confirmed the presence of encapsulated C_{60} and C_{70} in these complexes.

The structures of **2**, $(C_{60})_3$⊂**2**, and $(C_{70})_2$⊂**2** were optimized by the PM6 method. The tetrafacial barrel **2** possesses a cavity large enough to accommodate three C_{60} or two C_{70} molecules (Figure S25). Inside the cavity of **2**, the three C_{60} molecules are linearly oriented along one diagonal (Figure 7a). This

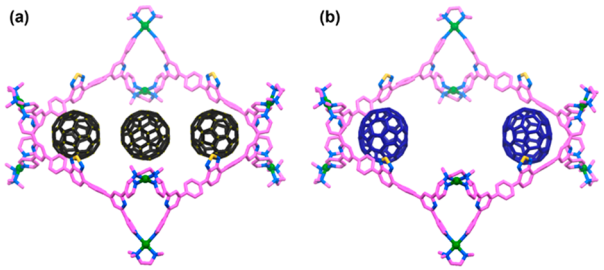

Figure 7. Optimized structures of (a) $(C_{60})_3$⊂**2** and (b) $(C_{70})_2$⊂**2**. Color codes: carbons of host (pink), nitrogen (blue), sulfur (yellow), palladium (green), carbons of C_{60} guest (black), carbons of C_{70} guest (deep blue). Hydrogen atoms are omitted for clarity.

explains the origin of two peaks corresponding to C_{60} in the ^{13}C NMR spectrum of $(C_{60})_3$⊂**2**. The two peripheral C_{60} molecules within the cavity of **2** are in a different chemical environment compared to the central C_{60} molecule, and thus, two time-averaged peaks of slightly different intensities are observed in the ^{13}C NMR spectrum (Figure 4b). The two C_{70} molecules are diagonally oriented within the cavity (Figure 7b). Presumably, the π–π interactions between the cluster of aromatic rings of terpyridine-based building blocks of host **2** and ellipsoidal C_{70} provide the maximum stabilization in two corners of **2**.

Next, competitive binding experiments were performed by treating **1** with excess C_{60} and C_{70} added simultaneously in a 1:1 ratio (4 equiv of each C_{60} and C_{70} was added to 1 equiv of **1** and mixture stirred at 70 °C for 12 h), and the results were monitored by ESI-MS. Interestingly, the peaks obtained correspond to C_{70} encapsulated barrel $(C_{70})_2$⊂**2** (Figure 8a). Again, when 4 equiv of C_{60} was added to the complex $(C_{70})_2$⊂**2**, no change was observed in mass spectrum, confirming the high stability and selectivity of $(C_{70})_2$⊂**2** (Figure 8b). However, when 4 equiv of C_{70} was added to

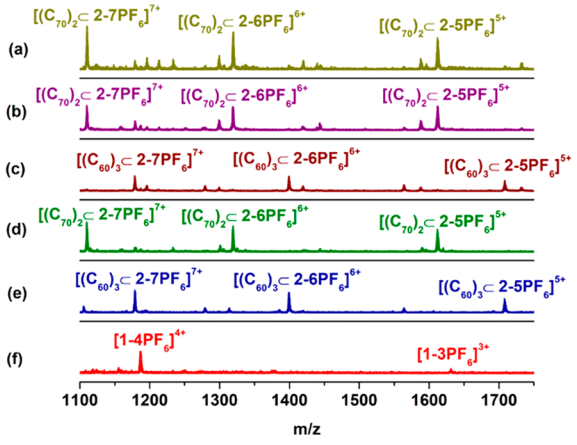

Figure 8. Partial stacked ESI-MS spectra: (a) after treatment of **1** with excess C_{60} and C_{70} (1:1 ratio), (b) after treatment of $(C_{70})_2$⊂**2** with excess C_{60}, (c) after treatment of $(C_{60})_3$⊂**2** with excess C_{70}, (d) $(C_{70})_2$⊂**2**, and (e) $(C_{60})_3$⊂**2** and (f) **1**.

https://doi.org/10.1021/jacsau.3c00224
JACS Au 2023, 3, 1998–2006

complex $(C_{60})_3$⊂**2**, C_{70} could not displace C_{60} molecules from the cavity of **2** (Figure 8c). These results imply that the barrel-to-barrel transformation occurs in the presence of both C_{60} and C_{70}. C_{70} has a slightly higher affinity toward the tetrafacial barrel (**2**); however, once three C_{60} molecules get encapsulated within the cavity of **2**, it forms the very stable host−guest complex $(C_{60})_3$⊂**2**, and C_{70} cannot replace the encapsulated C_{60} molecules from the cavity.

It was important to extract the fullerenes from the host−guest complexes to check the fate of the barrel. After screening with different solvents, 1,2-dichlorobenzene was found to be appropriate for the extraction experiments since barrel/host−guest complexes and fullerenes (C_{60}/C_{70}) have orthogonal solubilities in this solvent. C_{60} and C_{70} were successfully extracted from the complexes as was indicated by the pale purple/brown coloration of the 1,2-dichlorobenzene extract in the respective cases. Furthermore, ESI-MS analyses confirmed the existence of only trifacial barrel **1** and not tetrafacial barrel **2** after extraction in both cases (Figure 9a,c).

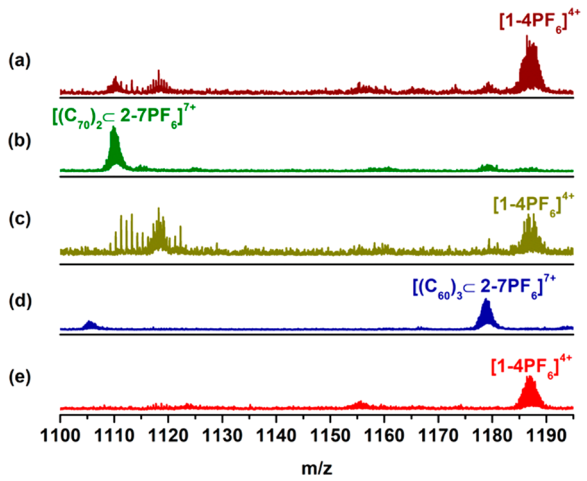

Figure 9. Partial stacked ESI-MS spectra: (a) after extraction of C_{70} from $(C_{70})_2$⊂**2** using 1,2-dichlorobenzene, (b) $(C_{70})_2$⊂**2**, (c) after extraction of C_{60} from $(C_{60})_3$⊂**2** using 1,2-dichlorobenzene, (d) $(C_{60})_3$⊂**2**, and (e) **1**.

This proves that the structural transformation from trifacial barrel to its higher homologue is feasible only in the presence of fullerenes. The removal of fullerenes from the host−guest complexes readily converted the tetrafacial barrel to the parent trifacial barrel in solution, which indicates that the tetrafacial barrel is a metastable form which can only exist in the presence of fullerenes (Scheme 2).

Singlet oxygen ($^1O_2$) generation is important for different uses. Photosensitizers upon light irradiation can transfer its absorbed energy to triplet oxygen to generate singlet oxygen. Fullerenes are well-known photosensitizers that can generate singlet oxygen, but their insolubility in common organic solvents limits their application. Good solubility of the PF_6^- analogues of $(C_{60})_3$⊂**2** and $(C_{70})_2$⊂**2** in acetonitrile prompted us to investigate the efficiencies of these complexes as photosensitizers for generating singlet oxygen using visible light. To the CD_3CN solutions of anthracene, 2 mol % of PF_6^- analogues of these complexes were added separately and irradiated with visible light, and the generation of singlet oxygen was monitored by the formation of anthracene endoperoxide over time using ^1H NMR. The complete

Scheme 2. Schematic Representation of Fullerene Induced Barrel to Barrel Transformation, Competitive Binding of C_{60} and C_{70}, and Fullerene Extraction

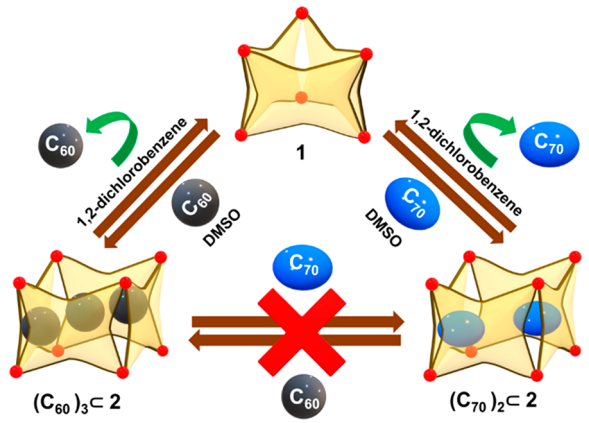

conversion of anthracene to anthracene-endoperoxide was achieved in 4 and 5 h using $(C_{70})_2$⊂**2** and $(C_{60})_3$⊂**2**, respectively (Figures S26 and S27). Although, $(C_{70})_2$⊂**2** has two molecules of fullerene, its slightly higher singlet oxygen generating ability compared to $(C_{60})_3$⊂**2** can be ascribed to its higher absorption in the visible region (Figure 6). The building block of free barrel **1**, $(C_{60})_3$⊂**2**, and $(C_{70})_2$⊂**2** contains a benzothiadiazole moiety which too is a photosensitizer. So, we also investigated the generation of singlet oxygen using 2 mol % of PF_6^- analogue of free barrel **1** as a photosensitizer in acetonitrile. Even after irradiation with visible light for 20 h, complete conversion of anthracene could not be achieved, thus showing the poor singlet oxygen generating ability of the free barrel **1** (Figures 10 and S28). Encapsulation of multiple fullerenes within the barrel enhanced singlet oxygen generation drastically (Figure 10). Notably, when an excess (20 mol %) of

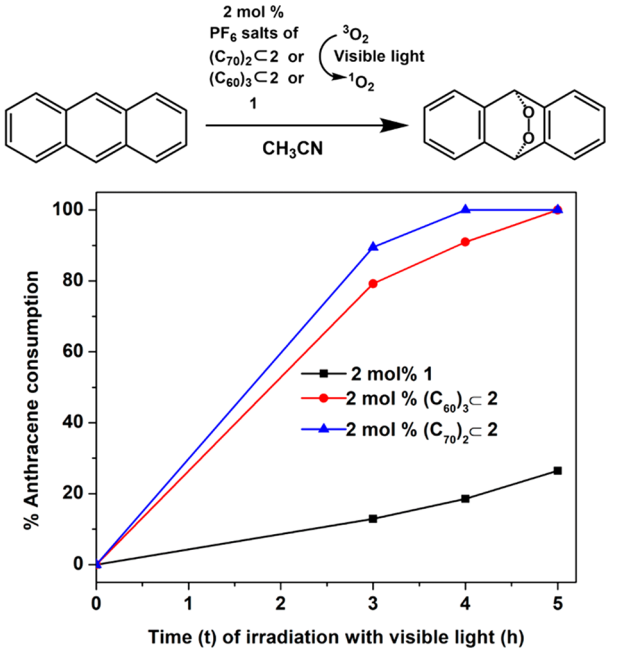

Figure 10. Comparison of singlet oxygen generating ability of $(C_{70})_2$⊂**2**, $(C_{60})_3$⊂**2**, and **1** obtained by monitoring anthracene consumption and formation of its endoperoxide over time upon visible light irradiation using ^1H NMR.

https://doi.org/10.1021/jacsau.3c00224
JACS Au 2023, 3, 1998−2006

either C_{70} or C_{60} was used as a heterogeneous photocatalyst for conversion of anthracene to its endoperoxide in acetonitrile, no conversion was observed (Figures S29 and S30), thus highlighting the importance of solubilizing fullerenes C_{60}/C_{70} in common organic solvents by encapsulation within a host for singlet oxygen generation.

CONCLUSIONS

In summary, we report here the synthesis of an adaptable trifacial molecular barrel (**1**) that undergoes structural change to a metastable higher homologue in the presence of suitable guests by efficient host−guest binding. The barrel (**1**) was obtained via self-assembly of a tetrapyridyl ligand **L** and a *cis*-blocked Pd(II) acceptor (**A**). The large cavity, open windows, and π-electron rich aromatic walls of **1** made it a potential candidate for electron deficient large guests like fullerenes C_{60} and C_{70}. The trifacial barrel (**1**) showed an uncommon structural transformation[70] to its metastable higher homologue tetrafacial barrel (**2**) in the presence of excess C_{60} and C_{70}, stabilizing three C_{60} and two C_{70} molecules in its enlarged cavity, respectively. Competitive binding experiments with C_{60} and C_{70} confirmed that C_{70} has a higher affinity for tetrafacial barrel **2** possibly due to greater π-interactions with the walls of the molecular barrel because of the ellipsoidal shape of C_{70}. The host−guest complexes $(C_{60})_3\subset$**2** and $(C_{70})_2\subset$**2** were thermodynamically stable and did not show guest exchange upon treatment with C_{70} and C_{60}, respectively. Trifacial barrel **1** was thus found to be a guest-responsive system which undergoes a structural expansion to a larger homologous molecular container to stabilize multiple fullerene molecules within its cavity. Further, the encapsulated fullerenes were extracted by washing with an appropriate solvent which led to the facile conversion of the metastable tetrafacial barrel to parent trifacial barrel **1**. Such a guest mediated reversible structural transformation between a 3D adaptable architecture and its higher homologue is an interesting observation. The PF_6^- analogues of $(C_{60})_3\subset$**2** and $(C_{70})_2\subset$**2** generated singlet oxygen under visible light irradiation in acetonitrile. The encapsulation of multiple fullerenes within host **2** was thus pivotal in solubilizing acetonitrile insoluble C_{60}/C_{70} molecules for acting as visible light photosensitizers in acetonitrile.

METHODS

All the chemicals were purchased from commercially available sources and used without further purification. NMR spectra were recorded on Bruker 400 and 500 MHz NMR spectrometers in DMSO-d_6. Electrospray ionization mass spectra (ESI-MS) were recorded using an Agilent 6538 Ultra-High Definition (UHD) Accurate Mass Q-TOF spectrometer using standard spectroscopic grade solvents. Electronic absorption spectra were recorded on a LAMBDA 750 UV/vis spectrophotometer. White LED (45 W) was used for singlet oxygen generation experiments.

The Gaussian 09 package was used for the computational study.[85] Trifacial barrel **1**, trifacial tube, tetrafacial barrel **2**, $(C_{60})_3\subset$**2**, and $(C_{70})_2\subset$**2** were optimized using the PM6 semiempirical method. No symmetry constraints were used during optimization.

ASSOCIATED CONTENT

Supporting Information

The Supporting Information is available free of charge at https://pubs.acs.org/doi/10.1021/jacsau.3c00224.

Experimental section, additional NMR spectra (^{1}H, COSY, NOESY, DOSY), mass spectra, optimized structures (PDF)

AUTHOR INFORMATION

Corresponding Author

Partha Sarathi Mukherjee − *Department of Inorganic and Physical Chemistry, Indian Institute of Science, Bangalore 560012, India;* orcid.org/0000-0001-6891-6697; Email: psm@iisc.ac.in

Authors

Ranit Banerjee − *Department of Inorganic and Physical Chemistry, Indian Institute of Science, Bangalore 560012, India*

Soumalya Bhattacharyya − *Department of Inorganic and Physical Chemistry, Indian Institute of Science, Bangalore 560012, India;* orcid.org/0000-0003-4467-6056

Complete contact information is available at: https://pubs.acs.org/10.1021/jacsau.3c00224

Author Contributions

‡R.B. and S.B. contributed equally. R.B. carried out the experimental works. S.B. carried out the optimization studies. R.B. and S.B. analyzed the experimental data. P.S.M. supervised the whole project. All authors contributed to writing this manuscript, and they have given approval to the final version of the manuscript. CRediT: **Ranit Banerjee** conceptualization, data curation, formal analysis, investigation, methodology, writing-original draft, writing-review & editing; **Soumalya Bhattacharyya** data curation, formal analysis, investigation, methodology, writing-original draft, writing-review & editing; **Partha Sarathi Mukherjee** conceptualization, funding acquisition, project administration, supervision, writing-original draft, writing-review & editing.

Notes

The authors declare no competing financial interest.

ACKNOWLEDGMENTS

P.S.M. thanks the SERB (New Delhi) for the research grant. R.B. gratefully acknowledges PMRF (India) for the research fellowship and contingency grant. The authors thank Mr. Pallab Bhandari and Mrs. Arppitha Baby Sainaba for help in recording mass spectra.

REFERENCES

(1) Caulder, D. L.; Brückner, C.; Powers, R. E.; König, S.; Parac, T. N.; Leary, J. A.; Raymond, K. N. Design, Formation and Properties of Tetrahedral M_4L_4 and M_4L_6 Supramolecular Clusters. *J. Am. Chem. Soc.* **2001**, *123*, 8923−8938.

(2) Yoshizawa, M.; Klosterman, J. K. Molecular architectures of multi-anthracene assemblies. *Chem. Soc. Rev.* **2014**, *43*, 1885−1898.

(3) Gao, W.-X.; Feng, H.-J.; Guo, B.-B.; Lu, Y.; Jin, G.-X. Coordination-Directed Construction of Molecular Links. *Chem. Rev.* **2020**, *120*, 6288−6325.

(4) Hardy, M.; Tessarolo, J.; Holstein, J. J.; Struch, N.; Wagner, N.; Weisbarth, R.; Engeser, M.; Beck, J.; Horiuchi, S.; Clever, G. H.; Lützen, A. A Family of Heterobimetallic Cubes Shows Spin-Crossover Behaviour Near Room Temperature. *Angew. Chem., Int. Ed.* **2021**, *60*, 22562−22569.

(5) Hasegawa, S.; Meichsner, S. L.; Holstein, J. J.; Baksi, A.; Kasanmascheff, M.; Clever, G. H. Long-Lived C_{60} Radical Anion

Stabilized Inside an Electron-Deficient Coordination Cage. *J. Am. Chem. Soc.* **2021**, *143*, 9718−9723.
(6) Seidel, S. R.; Stang, P. J. High-Symmetry Coordination Cages via Self-Assembly. *Acc. Chem. Res.* **2002**, *35*, 972−983.
(7) Fujita, M.; Tominaga, M.; Hori, A.; Therrien, B. Coordination Assemblies from a Pd(II)-Cornered Square Complex. *Acc. Chem. Res.* **2005**, *38*, 369−378.
(8) Saha, R.; Mondal, B.; Mukherjee, P. S. Molecular Cavity for Catalysis and Formation of Metal Nanoparticles for Use in Catalysis. *Chem. Rev.* **2022**, *122*, 12244−12307.
(9) Li, Y.; Jiang, Z.; Wang, M.; Yuan, J.; Liu, D.; Yang, X.; Chen, M.; Yan, J.; Li, X.; Wang, P. Giant, Hollow 2D Metalloarchitecture: Stepwise Self-Assembly of a Hexagonal Supramolecular. *Nut. J. Am. Chem. Soc.* **2016**, *138*, 10041−10046.
(10) Nitschke, J. R. Construction, Substitution, and Sorting of Metallo-organic Structures via Subcomponent Self-Assembly. *Acc. Chem. Res.* **2007**, *40*, 103−112.
(11) Debata, N. B.; Tripathy, D.; Chand, D. K. Self-assembled coordination complexes from various palladium(II) components and bidentate or polydentate ligands. *Coord. Chem. Rev.* **2012**, *256*, 1831−1945.
(12) Bloch, W. M.; Holstein, J. J.; Dittrich, B.; Hiller, W.; Clever, G. H. Hierarchical Assembly of an Interlocked M_8L_{16} Container. *Angew. Chem., Int. Ed.* **2018**, *57*, 5534−5538.
(13) Yu, G.; Yu, S.; Saha, M. L.; Zhou, J.; Cook, T. R.; Yung, B. C.; Chen, J.; Mao, Z.; Zhang, F.; Zhou, Z.; Liu, Y.; Shao, L.; Wang, S.; Gao, C.; Huang, F.; Stang, P. J.; Chen, X. A discrete organoplatinum (II) metallacage as a multimodality theranostic platform for cancer photochemotherapy. *Nat. Commun.* **2018**, *9*, 4335.
(14) Wang, H.; Wang, K.; Xu, Y.; Wang, W.; Chen, S.; Hart, M.; Wojtas, L.; Zhou, L.-P.; Gan, L.; Yan, X.; Li, Y.; Lee, J.; Ke, X.-S.; Wang, X.-Q.; Zhang, C.-W.; Zhou, S.; Zhai, T.; Yang, H.-B.; Wang, M.; He, J.; Sun, Q.-F.; Xu, B.; Jiao, Y.; Stang, P. J.; Sessler, J. L.; Li, X. Hierarchical Self-Assembly of Nanowires on the Surface by Metallo-Supramolecular Truncated Cuboctahedra. *J. Am. Chem. Soc.* **2021**, *143*, 5826−5835.
(15) Stefankiewicz, A. R.; Wałęsa-Chorab, M.; Harrowfield, J.; Kubicki, M.; Hnatejko, Z.; Korabik, M.; Patroniak, V. Self-assembly of transition metal ion complexes of a hybrid pyrazine-terpyridine ligand. *Dalton Trans.* **2013**, *42*, 1743−1751.
(16) Kilbas, B.; Mirtschin, S.; Scopelliti, R.; Severin, K. A solvent-responsive coordination cage. *Chem. Sci.* **2012**, *3*, 701−704.
(17) Henkelis, J. J.; Fisher, J.; Warriner, S. L.; Hardie, M. J. Solvent-Dependent Self-Assembly Behaviour and Speciation Control of Pd_6L_8 Metallo-supramolecular Cages. *Chem. -Eur. J.* **2014**, *20*, 4117−4125.
(18) Matsumoto, K.; Kusaba, S.; Tanaka, Y.; Sei, Y.; Akita, M.; Aritani, K.; Haga, M.-a.; Yoshizawa, M. A Peanut-Shaped Polyaromatic Capsule: Solvent-Dependent Transformation and Electronic Properties of a Non-Contacted Fullerene Dimer. *Angew. Chem., Int. Ed.* **2019**, *58*, 8463−8467.
(19) Kumar, A.; Banerjee, R.; Zangrando, E.; Mukherjee, P. S. Solvent and Counteranion Assisted Dynamic Self-Assembly of Molecular Triangles and Tetrahedral Cages. *Inorg. Chem.* **2022**, *61*, 2368−2377.
(20) Xie, T.-Z.; Endres, K. J.; Guo, Z.; Ludlow, J. M.; Moorefield, C. N.; Saunders, M. J.; Wesdemiotis, C.; Newkome, G. R. Controlled Interconversion of Superposed-Bistriangle, Octahedron, and Cuboctahedron Cages Constructed Using a Single, Terpyridinyl-Based Polyligand and Zn^{2+}. *J. Am. Chem. Soc.* **2016**, *138*, 12344−12347.
(21) Davies, J. A.; Ronson, T. K.; Nitschke, J. R. Twisted rectangular subunits self-assemble into a ferritin-like capsule. *Chem.* **2022**, *8*, 1099−1106.
(22) Cullen, W.; Hunter, C. A.; Ward, M. D. An Interconverting Family of Coordination Cages and a meso-Helicate; Effects of Temperature, Concentration, and Solvent on the Product Distribution of a Self-Assembly Process. *Inorg. Chem.* **2015**, *54*, 2626−2637.
(23) Shi, W.-J.; Liu, D.; Li, X.; Bai, S.; Wang, Y.-Y.; Han, Y.-F. Supramolecular Coordination Cages Based on N-Heterocyclic Carbene-Gold(I) Ligands and Their Precursors: Self-Assembly, Structural Transformation and Guest-Binding Properties. *Chem. -Eur. J.* **2021**, *27*, 7853−7861.
(24) Lewis, J. E. M.; Gavey, E. L.; Cameron, S. A.; Crowley, J. D. Stimuli-responsive Pd_2L_4 metallosupramolecular cages: towards targeted cisplatin drug delivery. *Chem. Sci.* **2012**, *3*, 778−784.
(25) Lisboa, L. S.; Findlay, J. A.; Wright, L. J.; Hartinger, C. G.; Crowley, J. D. A Reduced-Symmetry Heterobimetallic $[PdPtL_4]^{4+}$ Cage: Assembly, Guest Binding, and Stimulus-Induced Switching. *Angew. Chem., Int. Ed.* **2020**, *59*, 11101−11107.
(26) Scherer, M.; Caulder, D. L.; Johnson, D. W.; Raymond, K. N. Triple Helicate—Tetrahedral Cluster Interconversion Controlled by Host-Guest Interactions. *Angew. Chem., Int. Ed.* **1999**, *38*, 1587−1592.
(27) Wood, D. M.; Meng, W.; Ronson, T. K.; Stefankiewicz, A. R.; Sanders, J. K. M.; Nitschke, J. R. Guest-Induced Transformation of a Porphyrin-Edged $Fe^{II}{}_4L_6$ Capsule into a $Cu^{I}Fe^{II}{}_2L_4$ Fullerene Receptor. *Angew. Chem., Int. Ed.* **2015**, *54*, 3988−3992.
(28) Wang, S.; Sawada, T.; Fujita, M. Capsule-bowl conversion triggered by a guest reaction. *Chem. Commun.* **2016**, *52*, 11653−11656.
(29) Wang, S.; Sawada, T.; Ohara, K.; Yamaguchi, K.; Fujita, M. Capsule-Capsule Conversion by Guest Encapsulation. *Angew. Chem., Int. Ed.* **2016**, *55*, 2063−2066.
(30) Yan, D.-N.; Cai, L.-X.; Cheng, P.-M.; Hu, S.-J.; Zhou, L.-P.; Sun, Q.-F. Photooxidase Mimicking with Adaptive Coordination Molecular Capsules. *J. Am. Chem. Soc.* **2021**, *143*, 16087−16094.
(31) Nishioka, Y.; Yamaguchi, T.; Yoshizawa, M.; Fujita, M. Unusual [2 + 4] and [2 + 2] Cycloadditions of Arenes in the Confined Cavity of Self-Assembled Cages. *J. Am. Chem. Soc.* **2007**, *129*, 7000−7001.
(32) Chi, X.; Tian, J.; Luo, D.; Gong, H.-Y.; Huang, F.; Sessler, J. L. Texas-Sized Molecular Boxes: From Chemistry to Applications. *Molecules* **2021**, *26*, 2426.
(33) Hastings, C. J.; Pluth, M. D.; Bergman, R. G.; Raymond, K. N. Enzymelike Catalysis of the Nazarov Cyclization by Supramolecular Encapsulation. *J. Am. Chem. Soc.* **2010**, *132*, 6938−6940.
(34) Murase, T.; Horiuchi, S.; Fujita, M. Naphthalene Diels-Alder in a Self-Assembled Molecular Flask. *J. Am. Chem. Soc.* **2010**, *132*, 2866−2867.
(35) Samanta, D.; Mukherjee, P. S. Multicomponent self-sorting of a Pd_7 molecular boat and its use in catalytic Knoevenagel condensation. *Chem. Commun.* **2013**, *49*, 4307−4309.
(36) Guo, J.; Xu, Y.-W.; Li, K.; Xiao, L.-M.; Chen, S.; Wu, K.; Chen, X.-D.; Fan, Y.-Z.; Liu, J.-M.; Su, C.-Y. Regio- and Enantioselective Photodimerization within the Confined Space of a Homochiral Ruthenium/Palladium Heterometallic Coordination Cage. *Angew. Chem., Int. Ed.* **2017**, *56*, 3852−3856.
(37) Das, P.; Kumar, A.; Howlader, P.; Mukherjee, P. S. A Self-Assembled Trigonal Prismatic Molecular Vessel for Catalytic Dehydration Reactions in Water. *Chem. -Eur. J.* **2017**, *23*, 12565−12574.
(38) Howlader, P.; Mondal, S.; Ahmed, S.; Mukherjee, P. S. Guest-Induced Enantioselective Self-Assembly of a Pd_6 Homochiral Octahedral Cage with a C_3-Symmetric Pyridyl Donor. *J. Am. Chem. Soc.* **2020**, *142*, 20968−20972.
(39) Shanmugaraju, S.; Mukherjee, P. S. Self-Assembled Discrete Molecules for Sensing Nitroaromatics. *Chem. -Eur. J.* **2015**, *21*, 6656−6666.
(40) Chowdhury, A.; Howlader, P.; Mukherjee, P. S. Aggregation-Induced Emission of Platinum(II) Metallacycles and Their Ability to Detect Nitroaromatics. *Chem. -Eur. J.* **2016**, *22*, 7468−7478.
(41) Zhang, M.; Saha, M. L.; Wang, M.; Zhou, Z.; Song, B.; Lu, C.; Yan, X.; Li, X.; Huang, F.; Yin, S.; Stang, P. J. Multicomponent Platinum(II) Cages with Tunable Emission and Amino Acid Sensing. *J. Am. Chem. Soc.* **2017**, *139*, 5067−5074.
(42) Li, Z.; Yan, X.; Huang, F.; Sepehrpour, H.; Stang, P. J. Near-Infrared Emissive Discrete Platinum(II) Metallacycles: Synthesis and Application in Ammonia Detection. *Org. Lett.* **2017**, *19*, 5728−5731.
(43) Purba, P. C.; Venkateswaralu, M.; Bhattacharyya, S.; Mukherjee, P. S. Silver(I)-Carbene Bond-Directed Rigidification-

https://doi.org/10.1021/jacsau.3c00224
JACS Au 2023, 3, 1998−2006

Induced Emissive Metallacage for Picric Acid Detection. *Inorg. Chem.* **2022**, *61*, 713−722.
(44) Chen, S.; Li, K.; Zhao, F.; Zhang, L.; Pan, M.; Fan, Y.-Z.; Guo, J.; Shi, J.; Su, C.-Y. A metal-organic cage incorporating multiple light harvesting and catalytic centres for photochemical hydrogen production. *Nat. Commun.* **2016**, *7*, 13169.
(45) Zhang, Z.; Zhao, Z.; Hou, Y.; Wang, H.; Li, X.; He, G.; Zhang, M. Aqueous Platinum(II)-Cage-Based Light-Harvesting System for Photocatalytic Cross-Coupling Hydrogen Evolution Reaction. *Angew. Chem., Int. Ed.* **2019**, *58*, 8862−8866.
(46) Acharyya, K.; Bhattacharyya, S.; Sepehrpour, H.; Chakraborty, S.; Lu, S.; Shi, B.; Li, X.; Mukherjee, P. S.; Stang, P. J. Self-Assembled Fluorescent Pt(II) Metallacycles as Artificial Light-Harvesting Systems. *J. Am. Chem. Soc.* **2019**, *141*, 14565−14569.
(47) Jia, P.-P.; Xu, L.; Hu, Y.-X.; Li, W.-J.; Wang, X.-Q.; Ling, Q.-H.; Shi, X.; Yin, G.-Q.; Li, X.; Sun, H.; Jiang, Y.; Yang, H.-B. Orthogonal Self-Assembly of a Two-Step Fluorescence-Resonance Energy Transfer System with Improved Photosensitization Efficiency and Photooxidation Activity. *J. Am. Chem. Soc.* **2021**, *143*, 399−408.
(48) Kumar, A.; Saha, R.; Mukherjee, P. S. Self-assembled metallasupramolecular cages towards light harvesting systems for oxidative cyclization. *Chem. Sci.* **2021**, *12*, 5319−5329.
(49) Acharyya, K.; Bhattacharyya, S.; Lu, S.; Sun, Y.; Mukherjee, P. S.; Stang, P. J. Emissive Platinum(II) Macrocycles as Tunable Cascade Energy Transfer Scaffolds. *Angew. Chem., Int. Ed.* **2022**, *61*, No. e202200715.
(50) Sepehrpour, H.; Fu, W.; Sun, Y.; Stang, P. J. Biomedically Relevant Self-Assembled Metallacycles and Metallacages. *J. Am. Chem. Soc.* **2019**, *141*, 14005−14020.
(51) Bhattacharyya, S.; Venkateswarulu, M.; Sahoo, J.; Zangrando, E.; De, M.; Mukherjee, P. S. Self-Assembled Pt^{II}_8 Metallosupramolecular Tubular Cage as Dual Warhead Antibacterial Agent in Water. *Inorg. Chem.* **2020**, *59*, 12690−12699.
(52) Bhattacharyya, S.; Ali, S. R.; Venkateswarulu, M.; Howlader, P.; Zangrando, E.; De, M.; Mukherjee, P. S. Self-Assembled Pd_{12} Coordination Cage as Photoregulated Oxidase-Like Nanozyme. *J. Am. Chem. Soc.* **2020**, *142*, 18981−18989.
(53) Li, G.; Yu, W.; Ni, J.; Liu, T.; Liu, Y.; Sheng, E.; Cui, Y. Self-Assembly of a Homochiral Nanoscale Metallacycle from a Metallosalen Complex for Enantioselective Separation. *Angew. Chem., Int. Ed.* **2008**, *47*, 1245−1249.
(54) Zhang, W.-Y.; Lin, Y.-J.; Han, Y.-F.; Jin, G.-X. Facile Separation of Regioisomeric Compounds by a Heteronuclear Organometallic Capsule. *J. Am. Chem. Soc.* **2016**, *138*, 10700−10707.
(55) Rajasekar, P.; Pandey, S.; Ferrara, J. D.; Del Campo, M.; Le Magueres, P.; Boomishankar, R. Chiral Separation of Styrene Oxides Supported by Enantiomeric Tetrahedral Neutral Pd(II) Cages. *Inorg. Chem.* **2019**, *58*, 15017−15020.
(56) Sainaba, A. B.; Venkateswarulu, M.; Bhandari, P.; Arachchige, K. S. A.; Clegg, J. K.; Mukherjee, P. S. An Adaptable Water-Soluble Molecular Boat for Selective Separation of Phenanthrene from Isomeric Anthracene. *J. Am. Chem. Soc.* **2022**, *144*, 7504−7513.
(57) Samanta, D.; Gemen, J.; Chu, Z.; Diskin-Posner, Y.; Shimon, L. J. W.; Klajn, R. Reversible photoswitching of encapsulated azobenzenes in water. *Proc. Natl. Acad. Sci. U.S.A.* **2018**, *115*, 9379−9384.
(58) Howlader, P.; Mondal, B.; Purba, P. C.; Zangrando, E.; Mukherjee, P. S. Self-Assembled Pd(II) Barrels as Containers for Transient Merocyanine Form and Reverse Thermochromism of Spiropyran. *J. Am. Chem. Soc.* **2018**, *140*, 7952−7960.
(59) Saha, R.; Devaraj, A.; Bhattacharyya, S.; Das, S.; Zangrando, E.; Mukherjee, P. S. Unusual Behavior of Donor-Acceptor Stenhouse Adducts in Confined Space of a Water-Soluble Pd^{II}_8 Molecular Vessel. *J. Am. Chem. Soc.* **2019**, *141*, 8638−8645.
(60) Bhat, I. A.; Jain, R.; Siddiqui, M. M.; Saini, D. K.; Mukherjee, P. S. Water-Soluble Pd_8L_4 Self-assembled Molecular Barrel as an Aqueous Carrier for Hydrophobic Curcumin. *Inorg. Chem.* **2017**, *56*, 5352−5360.
(61) Bhandari, P.; Modak, R.; Bhattacharyya, S.; Zangrando, E.; Mukherjee, P. S. Self-Assembly of Octanuclear Pt^{II}/Pd^{II} Coordination Barrels and Uncommon Structural Isomerization of a Photochromic Guest in Molecular Space. *JACS Au* **2021**, *1*, 2242−2248.
(62) Castro, E.; Murillo, J.; Fernandez-Delgado, O.; Echegoyen, L. Progress in fullerene-based hybrid perovskite solar cells. *J. Mater. Chem. C* **2018**, *6*, 2635−2651.
(63) Lucas, S.; Leydecker, T.; Samorì, P.; Mena-Osteritz, E.; Bäuerle, P. Covalently linked donor-acceptor dyad for efficient single material organic solar cells. *Chem. Commun.* **2019**, *55*, 14202−14205.
(64) Lee, Y. W.; Yeop, J.; Lim, H.; Park, W.-W.; Joung, J. F.; Park, S.; Kwon, O.-H.; Kim, J. Y.; Woo, H. Y. Fullerene-Based Triads with Controlled Alkyl Spacer Length as Photoactive Materials for Single-Component Organic Solar Cells. *ACS Appl. Mater. Interfaces* **2021**, *13*, 43174−43185.
(65) Campidelli, S.; Vázquez, E.; Milic, D.; Lenoble, J.; Atienza Castellanos, C.; Sarova, G.; Guldi, D. M.; Deschenaux, R.; Prato, M. Liquid-Crystalline Bisadducts of [60]Fullerene. *J. Org. Chem.* **2006**, *71*, 7603−7610.
(66) Yamakoshi, Y.; Umezawa, N.; Ryu, A.; Arakane, K.; Miyata, N.; Goda, Y.; Masumizu, T.; Nagano, T. Active Oxygen Species Generated from Photoexcited Fullerene (C_{60}) as Potential Medicines: $O_2^{-\bullet}$ versus $^1O_2$. *J. Am. Chem. Soc.* **2003**, *125*, 12803−12809.
(67) Castro, E.; Garcia, A. H.; Zavala, G.; Echegoyen, L. Fullerenes in biology and medicine. *J. Mater. Chem. B* **2017**, *5*, 6523−6535.
(68) Hirsch, A.; Lamparth, I.; Karfunkel, H. R. Fullerene Chemistry in Three Dimensions: Isolation of Seven Regioisomeric Bisadducts and Chiral Trisadducts of C_{60} and Di(ethoxycarbonyl)methylene. *Angew. Chem., Int. Ed. Engl.* **1994**, *33*, 437−438.
(69) García-Simón, C.; Garcia-Borràs, M.; Gómez, L.; Parella, T.; Osuna, S.; Juanhuix, J.; Imaz, I.; Maspoch, D.; Costas, M.; Ribas, X. Sponge-like molecular cage for purification of fullerenes. *Nat. Commun.* **2014**, *5*, 5557.
(70) Banerjee, R.; Chakraborty, D.; Jhang, W.-T.; Chan, Y.-T.; Mukherjee, P. S. Structural Switching of a Distorted Trigonal Metal-Organic Cage to a Tetragonal Cage and Singlet Oxygen Mediated Oxidations. *Angew. Chem., Int. Ed.* **2023**, No. e202305338.
(71) Brenner, W.; Ronson, T. K.; Nitschke, J. R. Separation and Selective Formation of Fullerene Adducts within an $M^{II}_8L_6$ Cage. *J. Am. Chem. Soc.* **2017**, *139*, 75−78.
(72) Chen, B.; Holstein, J. J.; Horiuchi, S.; Hiller, W. G.; Clever, G. H. Pd(II) Coordination Sphere Engineering: Pyridine Cages, Quinoline Bowls, and Heteroleptic Pills Binding One or Two Fullerenes. *J. Am. Chem. Soc.* **2019**, *141*, 8907−8913.
(73) Fuertes-Espinosa, C.; García-Simón, C.; Pujals, M.; Garcia-Borràs, M.; Gómez, L.; Parella, T.; Juanhuix, J.; Imaz, I.; Maspoch, D.; Costas, M.; Ribas, X. Supramolecular Fullerene Sponges as Catalytic Masks for Regioselective Functionalization of C_{60}. *Chem.* **2020**, *6*, 169−186.
(74) Purba, P. C.; Maity, M.; Bhattacharyya, S.; Mukherjee, P. S. A Self-Assembled Palladium(II) Barrel for Binding of Fullerenes and Photosensitization Ability of the Fullerene-Encapsulated Barrel. *Angew. Chem., Int. Ed.* **2021**, *60*, 14109−14116.
(75) Cai, L.-X.; Yan, D.-N.; Cheng, P.-M.; Xuan, J.-J.; Li, S.-C.; Zhou, L.-P.; Tian, C.-B.; Sun, Q.-F. Controlled Self-Assembly and Multistimuli-Responsive Interconversions of Three Conjoined Twin-Cages. *J. Am. Chem. Soc.* **2021**, *143*, 2016−2024.
(76) Tsutsui, T.; Catti, L.; Yoza, K.; Yoshizawa, M. An atropisomeric M_2L_4 cage mixture displaying guest-induced convergence and strong guest emission in water. *Chem. Sci.* **2020**, *11*, 8145−8150.
(77) Rizzuto, F. J.; Nitschke, J. R. Stereochemical plasticity modulates cooperative binding in a $Co^{II}_{12}L_6$ cuboctahedron. *Nat. Chem.* **2017**, *9*, 903−908.
(78) Percástegui, E. G. Guest-Induced Transformations in Metal-Organic Cages. *Eur. J. Inorg. Chem.* **2021**, *2021*, 4425−4438.
(79) Yazaki, K.; Akita, M.; Prusty, S.; Chand, D. K.; Kikuchi, T.; Sato, H.; Yoshizawa, M. Polyaromatic molecular peanuts. *Nat. Commun.* **2017**, *8*, 15914.

https://doi.org/10.1021/jacsau.3c00224
JACS Au 2023, 3, 1998−2006

(80) Wu, D.; Shao, T.; Men, J.; Chen, X.; Gao, G. Superaromatic terpyridines based on corannulene responsive to metal ions. *Dalton Trans.* **2014**, *43*, 1753−1761.
(81) Gorczyński, A.; Harrowfield, J. M.; Patroniak, V.; Stefankiewicz, A. R. Quaterpyridines as Scaffolds for Functional Metallosupramolecular Materials. *Chem. Rev.* **2016**, *116*, 14620−14674.
(82) Dou, C.; Chen, D.; Iqbal, J.; Yuan, Y.; Zhang, H.; Wang, Y. Multistimuli-Responsive Benzothiadiazole-Cored Phenylene Vinylene Derivative with Nanoassembly Properties. *Langmuir* **2011**, *27*, 6323−6329.
(83) Saraswati, T. E.; Setiawan, U. H.; Ihsan, M. R.; Isnaeni, I.; Herbani, Y. The Study of the Optical Properties of C_{60} Fullerene in Different Organic Solvents. *Open Chem.* **2019**, *17*, 1198−1212.
(84) Sachdeva, S.; Singh, D.; Tripathi, S. K. Optical and electrical properties of fullerene C_{70} for solar cell applications. *Opt. Mater.* **2020**, *101*, 109717.
(85) Frisch, M. J.; Trucks, G. W.; Schlegel, H. B.; Scuseria, G. E.; Robb, M. A.; Cheeseman, J. R.; Scalmani, G.; Barone, V.; Mennucci, B.; Petersson, G. A.; Nakatsuji, H.; Caricato, M.; Li, X.; Hratchian, H. P.; Izmaylov, A. F.; Bloino, J.; Zheng, G.; Sonnenberg, J. L.; Hada, M.; Ehara, M.; Toyota, K.; Fukuda, R.; Hasegawa, J.; Ishida, M.; Nakajima, T.; Honda, Y.; Kitao, O.; Nakai, H.; Vreven, T.; Montgomery, Jr., J. A.; Peralta, J. E.; Ogliaro, F.; Bearpark, M.; Heyd, J. J.; Brothers, E.; Kudin, K. N.; Staroverov, V. N.; Kobayashi, R.; Normand, J.; Raghavachari, K.; Rendell, K. A.; Burant, J. C.; Iyengar, S. S.; Tomasi, J.; Cossi, M.; Rega, N.; Millam, J. M.; Klene, M.; Knox, J. E.; Cross, J. B.; Bakken, V.; Adamo, C.; Jaramillo, J.; Gomperts, R.; Stratmann, R. E.; Yazyev, O.; Austin, A. J.; Cammi, R.; Pomelli, C.; Ochterski, J. W.; Martin, R. L.; Morokuma, K.; Zakrzewski, V. G.; Voth, G. A.; Salvador, P.; Dannenberg, J. J.; Dapprich, S.; Daniels, A. D.; Farkas, D6.; Foresman, J. B.; Ortiz, J. V.; Cioslowski, J.; Fox, D. J. *Gaussian 09*, Revision d.01; Gaussian. Inc.: Wallingford, CT, 2009.

https://doi.org/10.1021/jacsau.3c00224
JACS Au 2023, 3, 1998−2006